PRAJÑĀ - **Journal of Pure and Applied Sciences Vol. 24 – 25 : 59 – 77 (2017)**
ISSN 0975 - 2595

EFFICIENT COUPLING OF A LASER DIODE TO A QUADRIC INTERFACE MICROLENS TIPPED CIRCULAR CORE PHOTONIC CRYSTAL FIBER WITH OPTIMIZATION OF STRUCTURE PARAMETER USING ABCD MATRIX FORMALISM

SUMANTA MUKHOPADHYAY
St. Paul's Cathedral Mission College, Department of Physics, 33/1 Raja Rammohan Roy Sarani, Kolkata-700009, West Bengal, India. E-mail: sumukherjee_74@yahoo.com

ABSTRACT

We theoretically investigate the coupling optics involving a laser diode emitting two wavelengths either 1.3 μm or 1.5 μm and a series of circular core photonic crystal fibers with different air filling ratio and hole-pitch via quadric interface microlens of six different focal lengths on the tip of such fibers. Instead of considering special ABCD matrix for individual microlens like hyperbolic, parabolic and elliptical (hemispherical included) one, a simple and accurate unified transfer ABCD matrix for refraction of quadric microlens under paraxial approximation is utilized to analyze the theoretical coupling efficiency, based on Gaussian beam approximation. Further, it is observed that, for a fit structure parameter of quadric interfaced microlens, photonic crystal fiber with air filling ratio of 0.35 and hole-pitch of 5.0 μm comes out to be the most suitable one to couple laser diode for both wavelengths of practical interest, specially that of light emitting wavelength $\lambda = 1.5\mu m$. ***Moreover, the coupling efficiency can reach to nearly 100 % with simultaneous optimization of structure parameter and focal length of specific lensed fiber. The analysis should find use in ongoing investigations for optimum launch optics for the design of quadric interface microlens on the tip of photonic crystal fiber.***

Keywords: ABCD matrix, Quadric interface-lensed fiber, Structure parameter, Circular core photonic crystal fiber.

INTRODUCTION

Photonic crystal fiber (PCF), also known as microstructured optical fiber, has proved to be one of the most promising member for present-day fiber optic communication system and thereby becoming a subject of growing interest in Research and Development (R&D) for scientists, technologists and researchers. PCF is actually a unique type of pure silica optical fiber [1-3] with an array of air holes running along the total length of the fiber, reminiscent of a crystal lattice, which gives to this type of fiber, its name. The core is created by omitting the central air hole of the structure (Figure 1). Depending upon the light-guiding mechanism, PCFs can be categorized into two main classes. The first one, air-guided hollow core PCF in which light is guided by the photonic band-gap (PBG) effect, a mechanism that does not require a higher refractive index in the core to confine and guide light. The PBG guidance effect relies on coherent backscattering of light into the core. If the frequency of the light is in the bandgap of two-dimensional photonic crystal formed by the periodic cladding, light is guided by the PBG effect. A PBG fiber has air holes in the core region surrounded by a solid silica cladding with microscopic air holes running along its total length. Different kinds of band gap PCFs such as low loss air core, all solid have been also designed which find important applications that include CO_2 laser beam transmission, gas sensing, etc.[4].

On the other hand, the second one, index-guided solid core PCF for which the lower effective refractive index of the surrounding holes creates the cladding and the light is confined to the central solid core as in conventional optical fibers (COFs) and guided by modified total internal reflection (MTIR) mechanism. The index-guiding fiber, has a solid core region surrounded by a solid silica cladding, with regularly distributed air holes in a periodic arrangement, whose effective refractive index depends on the ratio of air to glass, also known as the air-fill ratio that comprises the structure. Due to the holes in the cladding region, the effective refractive index of the cladding region is reduced, which will provide the refractive index variation necessary to support total internal reflection at core cladding interface. Therefore, the light is confined to the

solid silica core, which has a relatively higher index than the effective cladding refractive index [4, 5]. Due to high design flexibility of PCFs compared to COFs, important optical properties can be tailored in PCFs [4, 5]. For index guiding solid core PCFs, these properties include endlessly single modeness, large mode area, high numerical aperture, high birefringence, high nonlinear coefficient and tailorable large dispersion [4]. Moreover, PCFs can transport light with very low loss in certain wavelength where COFs possess very large loss [5].

In some applications, preserving the state of polarization in fiber is important, particularly, this is essential in coherent optical communications and some specific fiber-optic sensors. The polarization state of the optical field can be maintained by introducing modal birefringence. Contrary to small achievable birefringence in COFs, high birefringence can be easily achieved in PCFs due to the large index contrast between core and cladding. The key technique is to destroy the symmetry of the structures of core and cladding. The structural symmetry of the core and cladding can be destroyed either by changing the shape or the size of the air holes near the core region or by changing both [4, 5]. Though the band gap PCF promises very large birefringence ($\sim 5.45\times10^{-2}$) at 1.55 μm [4], the birefringence of the index guided PCF yields also a very large value ($\sim 2.22 \times 10^{-2}$) [5] at same wavelength of light**.** Both types of fibers could be useful in designing fiber optic sensors which rely on fiber birefringence. The high value of birefringence will be useful in maintaining the polarization of electric fields, thus, making these fibers attractive in the fabrication of different fiber optic sensors such as temperature, humidity, pressure, strain, acoustic wave etc. These fibers may be also useful in the fabrication of polarization controllers [4, 5]. Moreover, band gap PCFs may be also useful in optical communications [4]. Bhattacharya and Konar have proposed a new type of index-guided PCF with triangular lattice of air holes which can be utilized for spectroscopy, biomedical application and supercontinuum generation [6]. Sharma et al. [7] have investigated a PCF which provides a moderate dispersion and large optical nonlinearity simultaneously, thereby their proposed PCF can act as a very efficient nonlinear medium for supercontinuum generation. The interest in supercontinuum generation is driven by several important applications such as optical metrology, optical coherence tomography, spectroscopy, wavelength division multiplexing and frequency comb generation [7]. Thus, in view of a wide range of optoelectronic applications of PCF in different sectors, the study of this special kind of optical fiber is of immense importance [8].

Now, one of the most recent and exciting developments in the field of photonics has been undoubtedly the fabrication of microlenses on the tip of optical fiber as far as coupling of a semiconductor laser diode (LD) to single mode fiber (SMF) is concerned. Actually, a wide range of photonic integrated semiconductor devices needs highly efficient, low-loss coupling which requires a gradual spot size transformation of the laser mode for the better compatibility of the wavefront and spot size of the laser beam to those of the guided mode in the fiber. Thus, optical packaging of semiconductor LD needs high coupling efficiencies and large misalignment tolerances from the viewpoint of its application based orientation for making the devices more rugged, more reliable and easier to handle. Moreover, the advantage of miniature and alignment free optical design between the microlens and the fiber, demands the fabrication of microlens on the tip of the fiber. The advantage of the design of more-compact optical components and modules also makes the design and fabrication of fiber microlens extremely attractive. Benefit of fiber sensing and optical recording also demands the use of fiber microlenses [9]. These microlenses, whether conical or hemispherical, possess the advantage of being self-centred. Such microlenses may have hyperbolic, hemispherical, parabolic, elliptic surfaces to modulate the spot size of LD light incident on them and transmit it into the SMF [10-22].

Now, it may be relevant to mention in this connection that the coupling optics involving hyperbolic microlens on the tip of the circular core step index single mode fiber (CCSISMF) [14, 15] as well as on the tip of circular core graded index single mode fiber (CCGISMF) [16] have been previously reported based on concerned ABCD matrix formalism [14, 15]. Moreover, the coupling optics

involving hemispherical microlens on the tip of CCSISMF [17] as well as on the tip of CCGISMF [18] in absence of transverse and angular misalignments have also been already reported based on concerned theoretical ABCD matrix model [17]. The coupling optics involving parabolic microlens on the tip of CCSISMF [19, 20] as well as on the tip of CCGISMF [21] have been recently reported based on very popular and relevant ABCD matrix formalism [19, 20].

Generally, fiber with hyperbolic, hemispherical, parabolic, elliptic microlens on its tip is nomenclatured as quadric interface lensed fiber of which structure parameter is an important generalized parameter for optimizing the coupling efficiency. The coupling optics involving quadric interface microlens (QIML) on the tip of CCSISMF [23, 24] as well as on the tip of CCGISMF [25] have been reported very recently based on concerned unified ABCD matrix formalism [23]. Moreover, in designing optimum launch optics involving such above mentioned microlenses like hyperbolic, hemispherical, parabolic, theoretical computations of such coupling efficiencies require cumbersome and lengthy numerical integrations [10-13]. The application of the ABCD system matrix formalism [14-25] for prediction of the excitation efficiency for coupling of a LD via different type of above-mentioned microlenses on the tip of different kinds of COFs has simplified calculations, nevertheless, yielding extremely accurate results [14-25]. Furthermore, calculations by this formalism are simple and executable with very little computation as well.

Thus, in the context of coupling optics there are considerable amount of research works on microlenses like hyperbolic, hemispherical, parabolic microlenses etc. on the tip different kinds of circular core COFs which have enriched the literature [10-25]. However, as per as R&Ds related with microlensing coupling schemes on the tip of circular core photonic crystal fibers (CCPCFs) are concerned, only a research paper investigating coupling of LD to solid core PCF via hyperbolic microlens has been reported very recently [26]. Though there are some research papers in literature related with quadric interfaced microlensing on the tip of different types of circular core COFs like CCSISMF [23, 24], CCGISMF [25], no such information is available regarding a study of coupling optics involving LD and CCPCF via QIML on the tip of the fiber. Moreover, the simplicity and effectiveness of method of computation of coupling optics of QIML involving ABCD matrix formalism [23-25] motivates us to concentrate on the present work, which aims the study of the coupling optics involving a LD via a QIML on the tip of CCPCF using relevant ABCD matrix [23-25]. Actually, it had been shown that prediction of the coupling optics in the case of a QIML on the tip of CCSISMF [23, 24] as well as on the tip of CCGISMF [25] have produced excellent results if we employ simple ABCD matrix formalism. Concerned calculations are executable with very little computations. It may be relevant to mention in this connection that in the case of a semiconductor LD emitting $1.3\mu m$ wavelength of light, uncoated QIMLs on the tip of a CCSISMF produce 99.87% coupling efficiency [23] i.e., an ideal LD having a symmetrical modal output and a QIML with an anti-reflection coating, has a theoretical coupling efficiency of nearly 100% [23]. Therefore, the effect of Fresnel backward reflection can be neglected in our requisite study of coupling optics. Such a study, which as per our knowledge, reported for the first time, should deserve the immediate attention of experimentalists.

In the first part of this paper, using simple, accurate and unified ABCD matrix formalism for refraction by a quadric interface [23, 24] we theoretically investigate the coupling efficiencies between a semiconductor LD emitting light of wavelength $\lambda = 1.3\ \mu m$ [12] and a series of CCPCFs with different air filling ratio d/Λ and hole pitch or lattice constant Λ [26] via QIML of six different focal parameters [23, 24] on the tip of these fibers in absence of possible transverse and angular mismatches. In the second part, we carry out the similar investigation for a LD emitting light of wavelength $\lambda = 1.5\ \mu m$ [12]. A comparison between these two cases is performed.

Further, we employ Gaussian field distributions for both the LD and the fiber. Experimentalists, system engineers and packagers would find these results appealing in designing CCPCFs with appropriate calibration, in the context of its simplicity compared to other

deeply involved rigorous methods like finite difference method (FDM) and finite element method (FEM). The present analysis, reported for the first time, contains significant new results in connection with the prediction of the suitable optogeometry of the QIML as well as that for the appropriate design of fiber geometry, i.e., core size, air hole pitch, size and the distribution of air holes, at a suitable wavelength emitted from the LD. The result will be extremely important for the designers and packagers who can, accordingly, mould and shape the desired QIML at the fiber end to achieve optimum coupling optics involving CCPCF in which air hole pitch, size, and distribution are additional degrees of freedom in comparison with the COFs.

THEORY AND ANALYSIS

Preview of fiber spot sizes of CCPCF

In our study, we consider an all-silica CCPCF having a triangular lattice of uniform structure for the air-hole of diameter d and glass matrix elongated along the entire length of the propagation direction of the fiber, as shown in Figure 1. The air-holes are distributed symmetrically around a central silica defect, which is actually an omitted air-hole, acting as the core of the said CCPCF. The infinite air-hole matrix with lattice-constant or hole-pitch Λ and air filling ratio d/Λ has been considered to act as the cladding of the CCPCF. Since the core-index n_{CO} is greater than that of the effective cladding index n_{FSM}, the fiber can guide light by the mechanism of MTIR as in case of a conventional step index fiber (CSF) [26, 27].

Now, the fundamental modal field in a CCPCF is approximated as a Gaussian function [26, 28] in the single mode region where air filling fraction of the PCF is smaller than 0.45 [29]

$$\psi_f = \exp\left[-\frac{x^2+y^2}{w_{eff}^2}\right] \tag{1}$$

where w_{eff} corresponds to the spot size of the CCPCF.

The upper and lower limits of the propagation constants β of the guided modes through the core of the CCPCF satisfy [8, 27]

$$k n_{CO} > \beta > \beta_{FSM} \tag{2}$$

where, $k=2\pi/\lambda$ being the wave number associated with the operating wavelength λ, n_{CO} is the refractive index of silica or the core material and β_{FSM} is the propagation constant of the fundamental space-filling mode (FSM), which is the fundamental mode in the infinite photonic crystal cladding without any defect or core.

The index corresponding to the FSM or the effective cladding index is [8, 27]

$$n_{FSM} = \frac{\beta_{FSM}}{k} \tag{3}$$

The procedure for obtaining the value of n_{FSM} for given parameters of the CCPCF at operating wavelength of light is detailed in Appendix A [26, 27]. Here all the coefficients are determined by applying the least square fitting method for the operating wavelengths $\lambda = 1.3\mu m$ and $\lambda = 1.5\mu m$, presented in Tables 1 and 2, respectively. These coefficients are utilized to determine the values of n_{FSM} of the CCPCF for various values of hole-pitch and the air filling ratio at any particular wavelength of interest [26].

The effective cladding index n_{FSM} can be used to find the effective *V*-parameter of the CCPCF, treating the CCPCF like a CSF, with its cladding and core indices same as those of infinite photonic crystal structure and silica, respectively. Now the effective *V* value of the CCPCF is given by [26, 27, 30, 31]

$$V_{eff} = \frac{2\pi}{\lambda} a_{eff} \left[n_{CO}^2 - n_{FSM}^2 \right]^{1/2} \tag{4}$$

where a_{eff} is the effective core radius which is assumed [26, 27, 30, 31] to be $\Lambda/\sqrt{3}$ and λ is the operating wavelength.

Then using Marcuse formula [28], the modal spot size w_{eff}, half of the mode field diameter (MFD) can be written as [26-28, 32]

$$\frac{w_{eff}}{a_{eff}} = 0.65 + \frac{1.619}{V_{eff}^{3/2}} + \frac{2.879}{V_{eff}^{6}} \tag{5}$$

The spot size of the CCPCF, w_{eff} is obtained by using Eq. (5), where V_{eff} being the effective *V*-parameter, calculated from Eq. (4). The method of such calculation has been detailed in Appendix A [26, 27].

Formulation of microlens coupling scheme

The coupling scheme to be studied is shown in Figure 1. Here, *L* is the separation distance in between the laser source and the nearest point of the QIML end of the fiber [23-25]. Our analysis is based on some usual approximations [10, 14-18, 20, 21, 23-26] like Gaussian field distributions for both the source and the fiber, no transmission loss, perfect matching of the polarisation mode of the fiber field, and that on the microlens surface, sufficient angular width of the microlens for ensuring the interception of entire power radiated by the source for typical values of the microlens parameters employed. However, since the spherical aberration is really determined by the properties of the microlens itself, its elimination is difficult by the said adjustment [33].

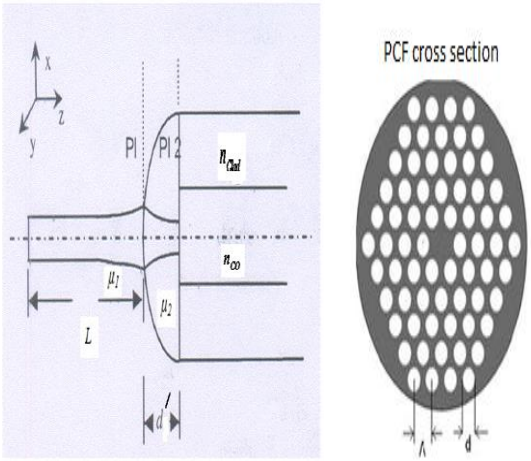

Figure 1. Geometry of LD to single mode CCPCF coupling via QIML on the tip of the fiber; μ_1 and μ_2 stand for refractive indices of incident and microlens media respectively.

The field Ψ_u representing the output of the LD at a distance *u* from the QIML surface is expressed by [23-25, 34-36]

$$\Psi_u = \exp\left[-\left(\frac{x^2}{w_{1x}^2}+\frac{y^2}{w_{1y}^2}\right)\right]\exp\left[-\frac{ik_1}{2}.\frac{x^2+y^2}{R_1}\right] \quad (6)$$

Here, elliptical intensity profiles of the laser beams are approximated by Gaussian spot sizes w_{1x} and w_{1y} along two mutually perpendicular directions, one perpendicular (X) and the other parallel (Y) to the junction planes, k_1 is the wave number in the incident medium and R_1 is the radius of curvature of the wavefronts from the LD. Our analysis is restricted to single frequency laser emitting only one spatial mode with a Gaussian intensity profile.

Moreover, it is already established that Gaussian approximations for the fundamental mode in circular core SMF [14-18, 20, 21, 23-26] sufficiently represent accurate results in the context of coupling losses for different types of microlensing schemes.

The QIML transformed laser field Ψ_v on the fiber plane 2 can be represented by [23-25, 34-36]

$$\Psi_v = \exp\left[-\left(\frac{x^2}{w_{2x}^2}+\frac{y^2}{w_{2y}^2}\right)\right]\exp\left[-\frac{ik_2}{2}\left(\frac{x^2}{R_{2x}}+\frac{y^2}{R_{2y}}\right)\right] \quad (7)$$

where w_{2x}, w_{2y} are, respectively, microlens transformed spot sizes, R_{2x}, R_{2y} being the respective transformed radii of curvature of the refracted wavefronts in the X and Y directions and k_2 is the wave number in the microlens medium. The method of finding w_{2x}, w_{2y}, R_{2x} and R_{2y} in terms of w_{1x}, w_{1y} and R_1 with the relevant ABCD matrix for QIML on the tip of the fiber is available in literature [23-25] and once again discussed in the Appendix B for ready reference. However, the different values of structure parameter *P* describe different structures of QIML like elliptical, hyperbolic, spherical and parabolic microlenses which are introduced in Table 3 [23-25].

The source to fiber coupling efficiency via QIML on the tip of the fiber is expressed in terms of well known overlap integral by [14-18, 20, 21, 23-26, 34-37]

$$\eta = \frac{\left|\iint \Psi_v \Psi_f^* dxdy\right|^2}{\iint |\Psi_v|^2 dxdy \iint |\Psi_f|^2 dxdy} \qquad (8)$$

Therefore η_0, the coupling efficiency in absence of misalignment, for CCPCF is given by [26]

$$\eta_0 = \frac{4w_{2x}w_{2y}w_{eff}^2}{\left[\left(w_{eff}^2 + w_{2x}^2\right)^2 + \frac{k_2^2 w_{2x}^4 w_{eff}^4}{4R_{2x}^2}\right]^{1/2}\left[\left(w_{2y}^2 + w_{eff}^2\right)^2 + \frac{k_2^2 w_{2y}^4 w_{eff}^4}{4R_{2y}^2}\right]^{1/2}} \qquad (9)$$

However, Eq. (9) can be obtained by employing Eqs. (1) and (7) in Eq. (8).

RESULTS AND DISCUSSION

Optogeometrical parameters under consideration

Our formalism employs the unified ABCD matrix under the paraxial approximation in order to predict the relevant coupling optics involving a LD and CCPCF via QIML on the tip of the fiber. For the estimation of coupling efficiencies in absence of any possible transverse and angular misalignments for a QIML of specific focal length on the tip of CCPCF, we firstly use a LD emitting light of wavelength $\lambda = 1.3\mu m$ with $w_{1x} = 1.081\mu m, w_{1y} = 1.161\mu m$ [12] and then LD emitting light of wavelength $\lambda = 1.5\mu m$ with $w_{1x} = 0.843\mu m$, $w_{1y} = 0.857\mu m$ [12]. The LD parameters used in this investigation are mentioned in Table 4. For the LD emitting light of abovementioned first wavelength, we study the coupling efficiencies for a series of CCPCFs having different air filling ratio d/Λ and hole-pitch or lattice-constant Λ [26] as mentioned in Tables 5(a) and 5(b). We choose three typical values of d/Λ, in the single moded region ($d/\Lambda \le 0.45$) corresponding to each arbitrary Λ value (Λ = 2.3, 3.0, 3.5, 4.0, 4.5, 5.0 μm), as 0.35, 0.40, 0.45 [26]. Different fiber spot sizes w_{eff} for these three d/Λ values corresponding to each Λ value (Λ = 2.3, 3.0, 3.5, 4.0, 4.5, 5.0 μm) [26] are then calculated [26, 27] and shown in Tables 5(a) and 5(b) where we also present the relevant structure parameters with corresponding maximum coupling efficiencies for $\lambda = 1.3\mu m$.

Following [14-18, 20, 21, 23-26] once again, the maximum depth of the microlens d' is taken as $6.0\,\mu m$ while the refractive index $\mu (= \mu_2 / \mu_1)$ of the material of the microlens with respect to surrounding medium is once again taken as 1.55. Further, since estimation of coupling efficiency on the basis of planar wave model for the input beam from the LD facet departs slightly from that on the basis of spherical wave model [14-18, 20, 21, 23-26], we consider planar wave model for the input beam from the LD facet for the sake of simplicity.

For the values of focal length (L) 7.6, 12.6, 17.6 [23] and 8.19, 12.1875, 16.19 [24] μm, respectively, we calculated the coupling efficiency varying with the structure parameter (P), and the results are shown in respective Tables 5(a) and 5(b). Then we use a LD emitting light of wavelength $\lambda = 1.5\mu m$ with $w_{1x} = 0.843\mu m, w_{1y} = 0.857\mu m$ [12]. We compute again relevant structure parameters with resulting maximum coupling efficiencies for the above same set used in the first part of this investigation and present them in Tables 6(a) and 6(b), respectively. The comparative optimized results of coupling efficiencies and coupling losses are shown in Table 7.

Results for coupling scheme without misalignment consideration

From Tables 5(a)-6(b), it is generally observed that the coupling efficiency can be improved through optimizing the structure parameter or in other words the structure parameter of the QIML is a key parameter that affects directly the coupling efficiency.

Now, it is observed from Tables 5(a) and 5(b) that the coupling efficiency can reach to 99.8334 % (i.e. coupling loss of 0.0072 dB) for a fit structure parameter (*P*) of 4.9 μm and a focal length (*L*) of 8.19 μm for the CCPCF with air filling ratio $d/\Lambda = 0.45$ and hole-pitch or lattice-constant $\Lambda = 4.5\mu m$ having spot size w_{eff} of 3.236339 μm, in case of excitation by a LD emitting light of abovementioned first wavelength. Moreover, from Tables 6(a) and 6(b), it is once again observed that for the fit structure parameter (*P*) of 4.3 μm, the maximum coupling efficiency can reach to 99.8423 % (i.e. coupling loss of 0.0068 dB) when L = 7.6 μm for the CCPCF with $d/\Lambda = 0.35$, $\Lambda = 5.0\mu m$ having corresponding spot size w_{eff} of 4.490145 μm, for excitation by a LD emitting light of abovementioned second wavelength.

It is seen from these Tables that for excitation by LDs emitting light of wavelengths $\lambda = 1.3\mu m$ and $\lambda = 1.5\mu m$, respectively, the maximum coupling efficiencies are nearly equal (99.8334% for CCPCF with $d/\Lambda = 0.45$, $\Lambda = 4.5\mu m$ having w_{eff} of 3.236339 μm for excitation by LD #1 and 99.8355 %, for CCPCF with $d/\Lambda = 0.35$, $\Lambda = 5.0\mu m$ having w_{eff} of 4.490145 μm for excitation by LD #2, respectively) for coupling by LDs via a QIML of identical focal length L = 8.19 μm on the tip of these respective fibers. Moreover, the structure parameters have a very little difference in case of such excitation by LDs emitting light of two wavelengths of practical interest (i.e. P = 4.9 μm for $\lambda = 1.3\mu m$ and P = 4.6 μm for $\lambda = 1.5\mu m$). It is also observed that, for excitation by a LD # 2 emitting light of wavelength $\lambda = 1.5\mu m$, the maximum coupling efficiency corresponds with CCPCFs with $d/\Lambda = 0.35$, $\Lambda = 5.0\mu m$ with w_{eff} of 4.490145 μm using QIML of all focal lengths proposed in our study. However, for excitation by LD # 1 emitting light of wavelength $\lambda = 1.3\mu m$, the coupling efficiency is once again maximum for CCPCFs with $d/\Lambda = 0.35$, $\Lambda = 5.0\mu m$ having w_{eff} of 4.433909 μm using QIML with all focal lengths used in our study except only two focal lengths L = 7.6 μm and 8.19 μm. Thus for identical values of fiber parameters of CCPCF with air filling ratio $d/\Lambda = 0.35$ and hole-pitch $\Lambda = 5.0\mu m$, the coupling efficiency can reach to nearly 100 % (99.6879 % for structure parameter P = 7.0 μm using QIML with focal length L= 12.1875 μm in case of excitation by LD # 1 emitting λ= 1.3 μm and 99.8423 % for structure parameter P = 4.3 μm using QIML with focal length L= 7.6 μm in case of excitation by LD # 2 emitting λ= 1.5 μm). Now, it may be relevant to mention in this connection that the wavelength at and around 1.5 μm is the region where the erbium doped fiber amplifier and Raman gain fiber amplifier operate efficiently and elegantly [16, 21]. Thus, the comparison between these results of maximum coupling efficiencies for the requisite CCPCF excited with two wavelengths predicts that CCPCFs with air filling ratio $d/\Lambda = 0.35$ and hole-pitch $\Lambda = 5.0\mu m$ are generally most suitable in the context of the aforesaid coupling optics involving CCPCFs for both wavelengths of practical interest and this excitement is uniquely excellent for excitation by a LD emitting specially light of wavelength $\lambda = 1.5\mu m$. Also it is revealed in our study that so far as the demand of achieving the merit of appreciable working distance to have maximum coupling efficiency on the tip of CCPCFs are concerned, this merit is acquired by CCPCF with $d/\Lambda = 0.35$ and $\Lambda = 5.0\mu m$. These values of V_{eff} for light of wavelengths $\lambda = 1.3\mu m$ and $\lambda = 1.5\mu m$, respectively, correspond to low V region which is very well known for evanescent wave coupling in optical fiber directional coupler.

For a typical estimation of knowledge of excitation via QIML with focal length (*L*) of 8.19 μm and 7.6 μm, respectively excited with LD # 1, 2 emitting light of wavelength $\lambda = 1.3\mu m$ and $\lambda = 1.5\mu m$, respectively we present the variation of coupling efficiencies versus the structure parameter for fibers

corresponding to $d/\Lambda = 0.45$, $\Lambda = 4.5\mu m$ with w_{eff} of 3.236339 μm and $d/\Lambda = 0.35$, $\Lambda = 5.0\mu m$ with w_{eff} of 4.490145 μm as shown in Figure 2. Figure 3 represents the variation of coupling efficiencies versus the structure parameter for fibers corresponding to $d/\Lambda = 0.45$, $\Lambda = 4.5\mu m$ with w_{eff} of 3.236339 μm and $d/\Lambda = 0.35$, $\Lambda = 5.0\mu m$ with w_{eff} of 4.490145 μm for excitation via QIML with identical focal length (L) of 8.19 μm, respectively excited with LD # 1, 2 emitting light of wavelength $\lambda = 1.3\mu m$ and $\lambda = 1.5\mu m$, respectively. However, in Figure 4, we have plotted the variation of coupling efficiencies versus the structure parameter for fibers corresponding to identical $d/\Lambda = 0.35$, $\Lambda = 5.0\mu m$ with w_{eff} of 4.433909 μm and 4.490145 μm, respectively for excitation via QIML with corresponding focal length (L) of 12.1875 μm and 7.6 μm, respectively excited with LD # 1, 2 emitting light of wavelength $\lambda = 1.3\mu m$ and $\lambda = 1.5\mu m$, respectively. In all of these figures, solid line (_____ denoting EFF0) corresponds to $\lambda = 1.3\mu m$, dashed line (---------- denoting EFF0DS) to $\lambda = 1.5\mu m$. We see that although the values of the typical structure parameters relevant with the maximum coupling efficiencies corresponding to curves are more or less the same, the optimum coupling efficiency is relatively better observed when the corresponding most suitable CCPCF is excited with LD #2 emitting light of wavelength $\lambda = 1.5\mu m$, in addition to the achievement of the appreciable working distance.

In CSFs, the single-mode optical bandwidth is typically limited by a higher-order mode cutoff at short wavelengths and macro-bend loss at long wavelengths [38]. On the other hand, the PCF can be designed to be endlessly single-mode (ESM), a term first coined by Birks et al. [8] referring to the fact that no higher-order modes are supported regardless of the wavelength. The ESM property has the specious consequence that the waveguide can be scaled to

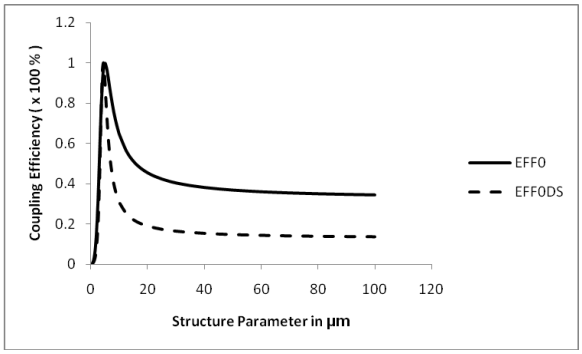

Figure 2. Variation of coupling efficiencies versus the structure parameter for fibers corresponding to $d/\Lambda = 0.45$, $\Lambda = 4.5\mu m$ with w_{eff} of 3.236339 μm and $d/\Lambda = 0.35$, $\Lambda = 5.0\mu m$ with w_{eff} of 4.490145 μm for excitation via QIML with focal length (L) of 8.19 and 7.6 μm, respectively excited with LD # 1, 2, emitting light of wavelength $\lambda = 1.3\mu m$ and $\lambda = 1.5\mu m$, respectively. Solid line (_____ denoting EFF0) corresponds to $\lambda = 1.3\mu m$, dashed line (---------- denoting EFF0DS) to $\lambda = 1.5\mu m$.

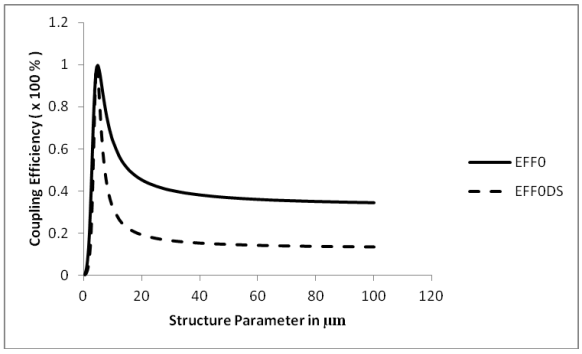

Figure 3. Variation of coupling efficiencies versus the structure parameter for fibers corresponding to $d/\Lambda = 0.45$, $\Lambda = 4.5\mu m$ with w_{eff} of 3.236339 μm and $d/\Lambda = 0.35$, $\Lambda = 5.0\mu m$ with w_{eff} of 4.490145 μm for excitation via QIML with identical focal length (L) of 8.19 μm, respectively excited with LD # 1, 2, emitting light of wavelength $\lambda = 1.3\mu m$ and $\lambda = 1.5\mu m$, respectively. Solid line (_____ denoting EFF0) corresponds to $\lambda = 1.3\mu m$, dashed line (---------- denoting EFF0DS) to $\lambda = 1.5\mu m$.

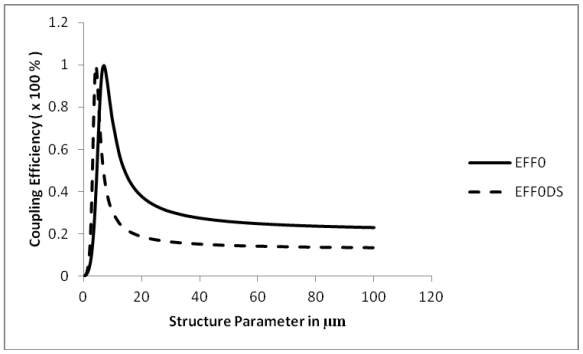

Figure 4. Variation of coupling efficiencies versus the structure parameter for fibers corresponding to identical $d/\Lambda = 0.35$, $\Lambda = 5.0\mu m$ with w_{eff} of 4.433909 μm and 4.490145 μm, respectively for excitation via QIML with corresponding focal length (L) of 12.1875 and 7.6 μm, respectively excited with LD # 1, 2, emitting light of wavelength $\lambda = 1.3\mu m$ and $\lambda = 1.5\mu m$, respectively. Solid line (_____ denoting EFF0) corresponds to $\lambda = 1.3\mu m$, dashed line (---------- denoting EFF0DS) to $\lambda = 1.5\mu m$.

an arbitrary dimension while remaining single mode [38]. Moreover, the PCF is found to have a significantly larger bandwidth than the CSF of an identical MFD as per as the measurements of the single-turn bend loss, spectral attenuation, etc. are concerned [38]. Recently PCFs with zero dispersion wavelengths around the 1.5 μm communications window have also been demonstrated [39]. This communication window provides efficient and elegant operation of erbium doped fiber amplifier and Raman gain fiber amplifier [16, 21]. However, it is observed in our present analysis that, for fit focal length of 8.19 μm of QIML on the tip CCPCF with air filling ratio of 0.45 and hole-pitch of 4.5 μm, the maximum coupling efficiency can reach to 99.8334 % for the structure parameter P = 4.9 μm in case of excitement by a LD emitting light of wavelength $\lambda = 1.3\mu m$. The corresponding value of coupling efficiency comes out to be 99.6879% for the structure parameter P = 7.0 μm using QIML of focal length L = 12.1875 μm on the tip of CCPCF with air filling ratio of 0.35 and hole-pitch of 5.0 μm in case of excitement by the same LD emitting light of wavelength $\lambda = 1.3\mu m$. It is observed generally that the respective value of the maximum coupling efficiency is 99.8423 % for fit focal length of 7.6 μm of QIML on the tip most efficient CCPCF with air filling ratio of 0.35 and hole-pitch of 5.0 μm, for the working distance P = 4.3 μm in case of excitement by a LD emitting light of wavelength $\lambda = 1.5\mu m$. Consequently the coupling losses, in absence of possible misalignments, have been reduced for excitement by a LD emitting light of wavelength $\lambda = 1.5\mu m$ in comparison with that obtained for excitement by a LD emitting light of wavelength $\lambda = 1.3\mu m$. Moreover, it is mentioned in Reference [40] that the additional design parameters of hole diameter d and hole-to-hole spacing Λ in CCPCF, enable much greater flexibility in the design of dispersion to suit the required application while in CSFs, group velocity dispersion is usually dominated by the dispersion of the bulk silica. Thus, our present analysis and results point out the merit of CCPCFs with specific air filling ratio of 0.35 and hole-pitch or lattice-constant of 5.0 μm in coupling by a LD emitting specially light of wavelength $\lambda = 1.5\mu m$ via hyperbolic microlens [26] as a special case of QIML of specific focal parameter on its tip. Although there is only a research paper involving experimental demonstration of efficient laser coupling through a hollow core PCF [41] in literature, there is limitation of availability of experimental research papers in the field of microlens coupling involving solid core PCFs. However, we are fortunate enough to compare our proposed results with those mentioned in the available literature [42] for the paraboloidal-shaped microlens etched from an SMF and fused on PCF having MFD of 11.1 μm excited by a LD of wavelength 1.31 μm. It is observed that our presented coupling scheme as a special case of QIML is in excellent agreement with those results mentioned in Reference [42]. Moreover, the excellent agreement of our results as special cases of QIML like hyperbolic microlens for CCPCF coupling in comparison with the available earlier theoretical results for coupling of CCPCF via such hyperbolic [26] microlens certifies the correctness of our simple formalism which is executable with little computations. We also conclude that structure parameter is not only the main factor to affect the maximum coupling efficiency. To acquire the maximum coupling efficiency, simultaneous optimization

of focal length and structure parameter is important**.**

Thus, it shows that once the structure parameters of QIML are optimized, the system designer will design appropriate microlens of suitable optogeometry according to their convenience. Hence, the method and results should find wide applications in prediction of optimal launch optics involving QIML, which has emerged as a potential candidate. Moreover, with the advent of new progress in nanotechnology, we are optimistic that the future technologist, will involve any breakthrough to reduce the dispersion values, associated with the wavelength 1.3 and 1.5 μm, by further optimization of the structure and better control of the fluctuations in fiber diameter and, ultimately realize and test our results of the above proposed theoretical formalism experimentally in near future.

CONCLUSION

The coupling optics involving LD to CCPCF excitation for different fiber parameters via QIML with different focal lengths on the tip of such fibers is theoretically formulated and investigated for the first time, to the best of our knowledge, in absence of possible transverse and angular mismatches. For a series of CCPCFs with different air filling ratio d/Λ and lattice-constant Λ, appropriate structure parameters are optimized so as to give maximum coupling efficiency for those respective fibers. Analytical expressions for the relevant quantities of practical interest are prescribed. Instead of considering special ABCD matrix for individual microlens like hyperbolic, hemispherical, elliptic and parabolic one, a unified expression for transfer ABCD matrix for refraction of QIML under paraxial approximation has been considered to simplify and execute the relevant calculations easily. The analysis will be extremely important and useful for the design of optimum launch optics in order to obtain maximum light coupling efficiency. The best maximum coupling is achieved for a CCPCF with air filling ratio of 0.35 and hole-pitch or lattice- constant of 5.0 μm when excited with LD emitting light of wavelength $\lambda = 1.3 \mu m$ and specially that of $\lambda = 1.5 \mu m$. Further, the importance of achieving appreciable structure parameter to have maximum coupling efficiency also stands in favour of the said CCPCF. For simplicity, we consider the two sources have same intensity profiles. It is observed from the standpoint of relevant coupling optics that LD emitting light of wavelength λ= 1.5 μm may be taken as a better alternative to source of wavelength λ= 1.3 μm as the lowest loss of window of glass corresponds with λ= 1.5 μm. But our data for λ= 1.3 μm is equally useful for such microlens coupling scheme. Moreover, simultaneous optimization of structure parameter and focal length is of immense importance in both the cases. In comparison with the other deeply involved rigorous methods like FEM and FDM, the application of novel unified ABCD matrix has simplified the analysis as the concerned calculations need very little computations. This methodology will be beneficial for the system engineers and packagers working in the field of optimum launch optics involving QIML on the tip of the CCPCF. Our study has the potential merit that once the structure parameters of QIML are optimized, the system designer will design appropriate microlens of suitable optogeometry in accordance with their convenience.

Appendix A

The usual normalized parameters u and v for the infinite cladding region of the chosen CCPCF are given by [2, 26, 27]

$$u = k\Lambda\left(n_{CO}^2 - \frac{\beta^2}{k^2}\right)^{1/2} \quad \text{(A1)}$$

and

$$v = k\Lambda\left(n_{CO}^2 - 1\right)^{1/2} \quad \text{(A2)}$$

with

$$u^2 + w^2 = v^2. \quad \text{(A3)}$$

In order to obtain the effective cladding index n_{FSM}, a basic air-hole at the centre of a hexagonal unit cell is approximated to a circle in a regular photonic crystal [8, 26, 27]. Then from relevant boundary conditions for the fields and their derivatives in terms of appropriate special functions, corresponding to a fixed value of v, obtained from Eq. (A2) for fixed Λ and λ - values, the concerned u values are computed for

different d / Λ values at a particular λ from the following Eq., taking n_{CO} = 1.45 [2, 26, 27]

$$wI_1(a_n w)\left[J_1(bu)Y_0(a_n u)-J_0(a_n u)Y_1(bu)\right] +uI_0(a_n w)\left[J_1(bu)Y_1(a_n u)-J_1(a_n u)Y_1(bu)\right]=0 \quad \text{(A4)}$$

where $a_n=\frac{d}{2\Lambda}$, $b=\left(\frac{\sqrt{3}}{2\pi}\right)^{1/2}$.

Using Eq. (A4), Russell has provided a polynomial fit to u, only for d/Λ = 0.4 and n_{CO} = 1.444. Further, for all d/Λ values of practical interest in the endlessly single mode region of a CCPCF, where d/Λ is less than 0.45, one should have a more general equation for wide applications [27].

The values of n_{FSM} are determined by replacing β/k in Eq. (A1) with n_{FSM} and this will lead to a modified simpler formulation of n_{FSM} as [26, 27]

$$n_{FSM}=A+B\left(\frac{d}{\Lambda}\right)+C\left(\frac{d}{\Lambda}\right)^2 \quad \text{(A5)}$$

where A, B and C are the three different optimization parameters, dependent on both the relative hole-diameter or hole-size d/Λ and the hole-pitch Λ.

Since optical communication window corresponds with two operating wavelengths of 1.3 μm and 1.5 μm, this study finds the coefficients for these two wavelengths of practical interest for different possible hole-pitches and hole-sizes of the CCPCF. Such modification in such a fitting is advantageous in the sense that it will help to reduce computation time since only nine coefficients are required in calculation instead of twenty seven coefficients [26, 27].

Now, for each value of Λ with the variations of d/Λ, the n_{FSM} values corresponding to respective u values obtained from Eq. (A4) are determined. Applying least square fitting of n_{FSM} in terms of d/Λ to Eq. (A5) for a particular Λ, the values of A, B and C can be then estimated. The various values of A, B and C are then simulated for different Λ in the endlessly single mode region of the CCPCF, resulting in the empirical relations of A, B and C in Eq. (A5), in terms of Λ, as given in the following [26, 27]

$$A=A_0+A_1\Lambda+A_2\Lambda^2 \quad \text{(A6)}$$

$$B=B_0+B_1\Lambda+B_2\Lambda^2 \quad \text{(A7)}$$

$$C=C_0+C_1\Lambda+C_2\Lambda^2 \quad \text{(A8)}$$

where A_i, B_i and C_i ($i=0,1$ and 2) are the optimization parameters for A, B and C, respectively. Computing A, B and C from Eqs. (A6-A8), one can find n_{FSM} directly for any d/Λ and Λ value at any particular λ using Eq. (A5) in the endlessly single mode region of the CCPCFs.

Appendix B

The relation between input and output parameters (q_1,q_2) of the light beam is given by

$$q_2=\frac{Aq_1+B}{Cq_1+D} \quad \text{(B1)}$$

where

$$\frac{1}{q_{1,2}}=\frac{1}{R_{1,2}}-\frac{i\lambda_0}{\pi w_{1,2}^2\mu_{1,2}} \quad \text{(B2)}$$

with symbols having their usual meanings as already described.

The ray matrix *M* for the QIML on the tip of the fiber is given by [23-25]

$$M=\begin{pmatrix}A & B\\ C & D\end{pmatrix}$$

$$M=\begin{pmatrix}1 & d'\\ 0 & 1\end{pmatrix}\begin{pmatrix}1 & 0\\ \frac{1-\mu}{\mu P} & \frac{1}{\mu}\end{pmatrix}\begin{pmatrix}1 & L\\ 0 & 1\end{pmatrix} \quad \text{(B3)}$$

where $A=1+\frac{d'(1-\mu)}{\mu P}$

$$B = L + \frac{(1-\mu)Ld'}{\mu P} + \frac{d'}{\mu}$$

$$C = \frac{1-\mu}{\mu P}$$

$$D = \frac{1}{\mu} + \frac{(1-\mu)L}{\mu P} \qquad \text{(B4)}$$

where d' is the maximum depth of the microlens, P is the structure parameter of the quadric interface lensed fiber, and L is the working distance which is also the distance of the LD from the microlens.

Again, the refractive index of the material of the microlens with respect to the surrounding medium is represented by $\mu(=\mu_2/\mu_1)$. The transformed beam spot sizes and radii of curvature in the X and Y directions are found by using expressions in Eq. (B4) in Eqs. (B1) and (B2) and can be expressed as

$$w_{2x,2y}^2 = \frac{A_1^2 w_{1x,1y}^2 + \dfrac{\left(\lambda_1^2 B^2\right)}{w_{1x,1y}^2}}{\mu(A_1 D - BC_1)} \qquad \text{(B5)}$$

$$\frac{1}{R_{2x,2y}} = \frac{A_1 C_1 w_{1x,1y}^2 + \dfrac{\left(\lambda_1^2 BD\right)}{w_{1x,1y}^2}}{A_1^2 w_{1x,1y}^2 + \dfrac{\left(\lambda_1^2 B^2\right)}{w_{1x,1y}^2}} \qquad \text{(B6)}$$

where

$$\lambda_1 = \frac{\lambda}{\pi}, \quad \lambda = \frac{\lambda_0}{\mu_1}, \quad A_1 = A + \frac{B}{R_1} \quad \text{and}$$

$$C_1 = C + \frac{D}{R_1}. \qquad \text{(B7)}$$

In plane wavefront model, the radius of curvature R_1 of the wavefront from the laser facet $\rightarrow\infty$. This leads to $A_1 = A$ and $C_1 = C$.

REFERENCES

[1] Russell, P. St. J. (2003) Photonic crystal fibers. *Science*, **299**: 358-362.

[2] Russell, P. St. J. (2006) Photonic-crystal fibers. *J. Lightwave Technol.*, **24**: 4729–4749.

[3] Bjarklev, A., Broeng, J. and Bjarklev, A. S. (2003) *Photonic Crystal Fibres*, Springer Science & Business Media Inc, NewYork.

[4] Bhattacharya, R. and Konar, S. (2012) Extremely large birefringence and shifting of zero dispersion wavelength of photonic crystal fibers. *Opt. & Laser Technol.*, **44**: 2210–2216.

[5] Sharma, M., Borogohain, N. and Konar, S. (2013) Index Guiding Photonic Crystal Fibers With Large Birefringence and Walk-Off. *J. Lightwave Technol.*, **31**: 3339-3344.

[6] Bhattacharya, R. and Konar, S. (2008) Design of a Photonic Crystal Fiber with Zero Dispersion Wavelength Near 0.65 µm. *Fiber and Integrated Opt.*, **27**: 89–98.

[7] Sharma, M., Konar, S. and Khan, K. R. (2015) Supercontinuum generation in highly nonlinear hexagonal photonic crystal fiber at very low power. *J. Nanophotonics*, **9**: 093073(1-8).

[8] Birks, T. A., Knight, J. C. and Russell, P. St. J. (1997) Endlessly single-mode photonic crystal fiber. *Opt. Lett.*, **22**: 961-963.

[9] Li, E. (2006) Characterization of fiber lens. *Opt. Lett.*, **31**: 169-171.

[10] Presby, H. M. and Edwards, C. A. (1992) Near 100% efficient fibre microlenses. *Electron. Lett.*, **28**: 582-584.

[11] Edwards, C. A., Presby, H. M. and Dragone, C. (1993) Ideal microlenses for laser to fiber coupling. *J. Lightwave Technol.*, **11**: 252-257.

[12] John, J., Maclean, T. S. M., Ghafouri-Shiraz, H. and Niblett, J. (1994) Matching of single-mode fibre to laser diode by microlenses at 1.5 μm wavelength. *IEE Proc. Optoelectron.*, **141**: 178-184.

[13] Presby, H. M. and Edwards, C. A. (1992) Efficient coupling of polarization maintaining fiber to laser diodes. *IEEE Photon. Technol. Lett.*, **4**: 897-899.

[14] Gangopadhyay, S. and Sarkar, S. N. (1996) Laser diode to single-mode fibre excitation via hyperbolic lens on the fibre tip: Formulation of ABCD matrix and efficiency computation. *Opt. Commun.*, **132**: 55-60.

[15] Gangopadhyay, S. and Sarkar, S. N. (1997) ABCD matrix for reflection and refraction of Gaussian light beams at surfaces of hyperboloid of revolution and efficiency computation for laser diode to single-mode fiber coupling by way of a hyperbolic lens on the fiber tip. *Appl. Opt.*, **36**: 8582-8586.

[16] Mukhopadhyay, S. and Sarkar, S. N. (2011) Coupling of a laser diode to single mode circular core graded index fiber via hyperbolic microlens on the fiber tip and identification of the suitable refractive index profile with consideration for possible misalignments. *Opt. Eng.*, **50**: 045004(1-9).

[17] Gangopadhyay, S. and Sarkar, S. N. (1998) Laser diode to single-mode fiber excitation via hemispherical lens on the fiber tip: Efficiency computation by ABCD matrix with consideration for allowable aperture. *J. Opt. Commun.*, **19**: 42-44.

[18] Bose, A., Gangopadhyay, S. and Saha, S. C. (2012) Laser diode to single mode circular core graded index fiber excitation via hemispherical microlens on the fiber tip: Identification of suitable refractive index profile for maximum efficiency with consideration for allowable aperture. *J. Opt. Commun.*, **33**: 15-19.

[19] Liu, H., Liu, L., Xu, R. and Luan, Z. (2005) ABCD matrix for reflection and refraction of Gaussian beams at the surface of a parabola of revolution. *Appl. Opt.*, **44**: 4809-4813.

[20] Liu, H. (2008) The approximate ABCD matrix for a parabolic lens of revolution and its application in calculating the coupling efficiency. *Optik*, **119**: 666-670.

[21] Mukhopadhyay, S. (2016) Coupling of a laser diode to single mode circular core graded index fiber via parabolic microlens on the fiber tip and identification of the suitable refractive index profile with consideration for possible misalignments. *J. Opt.*, **45**: 312–323.

[22] Massey, G. A. and Siegman, A. E. (1969) Reflection and refraction of Gaussian light beams at tilted ellipsoidal surfaces. *Appl. Opt.*, **8**: 975-978.

[23] Huang, J. and Yang, H. J. (2010) ABCD matrix model of quadric interface-lensed fiber and its application in coupling efficiency calculation. *Optik*, **121**: 531-534.

[24] Keshavarz, A. and Kazempour, M. (2012) Numerical calculation of coupling efficiency for an elegant Hermite-Cosh-Gaussian beams. *International J. of optics and Photonics*, **6**: 75-82.

[25] Mukhopadhyay, S. (2017) Laser diode to circular core graded index single mode fiber excitation via quadric interface microlens on the fiber tip and identification of the suitable refractive index profile for maximum coupling efficiency with optimization of structure parameter. *J Opt.*, **46**:359–367.

[26] Karak, A., Kundu, D., Mukhopadhyay, S. and Sarkar, S. N. (2015) Investigation of coupling of a laser diode to photonic crystal fiber via hyperbolic microlens on the fiber tip by ABCD matrix formalism. *Opt. Eng.*, **54**: 086102(1-7).

[27] Kundu, D. and Sarkar, S. (2014) Prediction of propagation characteristics of photonic crystal fibers by a simpler, more complete and versatile formulation of their effective cladding indices. *Opt. Eng.*, **53**: 056111(1-6).

[28] Marcuse, D. (1977) Loss analysis of single-mode fiber splices. *J. Bell Syst. Tech.*, **56**: 703–718.

[29] Hirooka, T., Hori, Y. and Nakazawa, M. (2004) Gaussian and sech approximations of mode field profiles in photonic crystal fibers. *IEEE Photon. Technol. Lett.*, **16**: 1071-1073.

[30] Koshiba, M. and Saitoh, K. (2004) Applicability of classical optical fiber theories to holey fibers. *Opt. Lett.*, **29**: 1739–1741.

[31] Saitoh, K. and Koshiba, M. (2005) Empirical relations for simple design of photonic crystal fibers. *Opt. Express*, **13**: 267-274.

[32] Ghatak, A. K. and Thyagarajan, K. (1998) *Introduction to Fiber Optics*, Cambridge University Press, United Kingdom.

[33] Bass, M. and Mahajan, V. N. (2010) *Handbook of Optics, in Geometrical and Physical Optics, Polarised Light, Components and Instruments*, McGraw-Hill, NewYork, Vol**.** 1, Edn. 3, Chapter 22 and Chapter 29.

[34] Sarkar, S. N., Thyagarajan, K. and Kumar, A. (1984) Gaussian approximation of the fundamental mode in single mode elliptic core fibers. *Opt. Commun.*, **49**: 178-183.

[35] Sarkar, S. N., Pal, B. P. and Thyagarajan, K. (1986) Lens coupling of laser diodes to monomode elliptic core fibers. *J. Opt. Commun.*, **7**: 92-96.

[36] Ghatak, A. K. and Thyagarajan, K. (1998) *Optical Electronics*, Cambridge University Press, United Kingdom, Chapter 13, pp 411-415.

[37] Sakai, J. and Kimura, T. (1980) Design of miniature lens for semiconductor laser to single mode fiber coupling. *IEEE J. Quantum Electron.*, **QE-16**: 1059–1066.

[38] Nielsen, M. D. , Folkenberg, J. R., Mortensen, N. A. and Bjarklev, A. (2004) Bandwidth comparison of photonic crystal fibers and conventional single mode fibers. *Opt. Express*, **12**: 430-435.

[39] Hansen, K. P., Jensen, J. R., Jacobsen, C., Simonsen, H. R., Broeng, J., Skovgaard, P. M. W., Peterson, A. and Bjarklev, A. (2002) Highly Nonlinear Photonic Crystal Fiber with Zero-Dispersion at 1.55μm. paper FA9 in *Optical Fiber Communication Conference 2002, Vol. **70** of OSA Trends in Optics and Photonics Series*, Optical Society of America, Washington, D.C..

[40] Reeves, W. H., Knight, J. C., Russell, P. St. .J. and Roberts, P. J. (2002) Demonstration of ultra-flattened dispersion in photonic crystal fibers. *Opt. Express***, 10**: 609- 613.

[41] Al-Janabi, A. H., Taher, H. J. and Laftah, S. M. (2011) Efficient transportation of Nd laser beam through photonic crystal fiber. *Indian J. Phys.*, **85**: 1299-1307.

[42] Peng, Z. S. and Wang, L. (2006) Optical coupling between a lensed photonic crystal fiber and a laser diode in *Int. Conf. on Communications, Circuits and Systems*, IEEE, Guilin.

Table 1: Values of all coefficients required for the formulation of effective cladding index n_{FSM} at $\lambda = 1.3\mu m$.

$\lambda = 1.3\mu m$			
	$i = 0$	$i = 1$	$i = 2$
A_i	1.430434	0.003803	-0.000214
B_i	0.069387	-0.012541	0.000650
C_i	-0.375746	0.107635	-0.008799

Table 2: Values of all coefficients required for the formulation of effective cladding index n_{FSM} at $\lambda = 1.5\mu m$.

$\lambda = 1.5\mu m$			
	$i = 0$	$i = 1$	$i = 2$
A_i	1.432783	0.002170	-0.000036
B_i	0.063468	-0.007890	0.000147
C_i	-0.415418	0.114257	-0.009127

Table 3: Structure parameters for different kinds of surface

Kinds of Surface	Mathematical Relation	Amount of Structure Parameter
Elliptical	$\frac{x^2}{a^2} + \frac{y^2}{b^2} = 1$	$P = \frac{b^2}{a}$
Hyperbolic	$\frac{x^2}{a^2} - \frac{y^2}{b^2} = 1$	$P = \frac{b^2}{a}$
Spherical	$x^2 + y^2 = r^2$	$P = r$
Parabolic	$x^2 = 2tz$	$P = t$

Table 4: Laser diode parameters

LD	Wavelength λ (μm)	Spot size w_{1x} (μm)	Spot size w_{1y} (μm)	λ_1 (μm)	k_2 (μm^{-1})
#1	1.3	1.081	1.161	0.4138	7.4915
#2	1.5	0.843	0.857	0.4775	6.4926

Table 5 (a):Results for optimum coupling efficiency for a series of CCPCFs with different air filling ratio d/Λ and hole-pitch or lattice-constant Λ via QIML with different focal lengths *L*, following Reference [23], at operating wavelength $\lambda = 1.3\mu m$. (*P* indicates structure parameter, w_{eff} indicates fiber spot size and η_0 indicates coupling coefficient without misalignment)

$d' = 6.0\ \mu m$, $\mu = 1.55$

d/Λ	Λ (μm)	w_{eff} (μm)	L = 7.6 μm		L = 12.6 μm		L = 17.6 μm	
			P(μm)	η_0	P(μm)	η_0	P(μm)	η_0
0.35	2.3	2.475538	4.2	0.971445	6.0	0.690619	7.7	0.454344
	3.0	2.744393	4.4	0.993208	6.4	0.760424	8.3	0.518478
	3.5	3.071572	4.6	0.997630	6.7	0.835083	8.8	0.595929
	4.0	3.482297	4.7	0.976379	6.9	0.908854	9.2	0.687721
	4.5	3.957274	4.7	0.926894	7.1	0.965260	9.5	0.781383
	5.0	4.433909	4.8	0.863142	7.2	0.993311	9.7	0.858528
0.40	2.3	2.106083	3.8	0.913878	5.2	0.588561	6.5	0.370322
	3.0	2.422810	4.2	0.965212	5.9	0.676283	7.5	0.441929
	3.5	2.740655	4.4	0.993026	6.4	0.759495	8.3	0.517582
	4.0	3.121711	4.6	0.996578	6.7	0.845315	8.9	0.607539
	4.5	3.553313	4.7	0.970427	7.0	0.919161	9.3	0.702685
	5.0	3.985642	4.7	0.923359	7.1	0.967701	9.5	0.786460
0.45	2.3	1.859907	3.5	0.861853	4.6	0.523169	5.5	0.320938
	3.0	2.191350	3.9	0.929727	5.5	0.612178	6.8	0.388939
	3.5	2.493922	4.2	0.973391	6.0	0.695539	7.7	0.458695
	4.0	2.845339	4.5	0.996920	6.5	0.784828	8.5	0.542585
	4.5	3.236339	4.6	0.992372	6.8	0.867485	9.0	0.633722
	5.0	3.627302	4.7	0.963599	7.0	0.929320	9.3	0.717923

Table 5 (b):Results for optimum coupling efficiency for a series of CCPCFs with different air filling ratio d/Λ and hole-pitch or lattice-constant Λ via QIML with different focal lengths *L*, following Reference [24], at operating wavelength $\lambda = 1.3\mu m$. (*P* indicates structure parameter, w_{eff} indicates fiber spot size and η_0 indicates coupling coefficient without misalignment)

$d' = 6.0\ \mu m, \mu = 1.55$

d/Λ	Λ (μm)	w_{eff} (μm)	$L = 8.19\mu m$		$L = 12.1875\mu m$		$L = 16.19\mu m$	
			P(μm)	η_0	P(μm)	η_0	P(μm)	η_0
0.35	2.3	2.475538	4.4	0.946862	5.9	0.714602	7.2	0.510379
	3.0	2.744393	4.6	0.979414	6.2	0.783506	7.8	0.577949
	3.5	3.071572	4.8	0.997517	6.5	0.855865	8.2	0.657715
	4.0	3.482297	4.9	0.991492	6.7	0.925266	8.6	0.749187
	4.5	3.957274	5.0	0.956133	6.9	0.975480	8.8	0.838185
	5.0	4.433909	5.0	0.902107	7.0	0.996879	9.0	0.906903
0.40	2.3	2.106083	4.0	0.876610	5.1	0.612378	6.1	0.419925
	3.0	2.422810	4.4	0.938650	5.8	0.700368	7.1	0.497149
	3.5	2.740655	4.6	0.979088	6.2	0.782605	7.8	0.577010
	4.0	3.121711	4.8	0.998321	6.6	0.865542	8.3	0.669481
	4.5	3.553313	4.9	0.987759	6.8	0.934756	8.6	0.763719
	5.0	3.985642	5.0	0.953331	6.9	0.977530	8.8	0.842846
0.45	2.3	1.859907	3.6	0.818513	4.5	0.546070	5.2	0.365880
	3.0	2.191350	4.1	0.895095	5.3	0.636190	6.4	0.440147
	3.5	2.493922	4.5	0.949598	5.9	0.719555	7.3	0.514993
	4.0	2.845339	4.7	0.987520	6.3	0.807316	7.9	0.603014
	4.5	3.236339	4.9	0.998334	6.6	0.886680	8.4	0.695812
	5.0	3.627302	4.9	0.983145	6.8	0.943965	8.7	0.778419

Table 6(a):Results for optimum coupling efficiency for a series of CCPCFs with different air filling ratio d/Λ and hole-pitch or lattice-constant Λ via QIML with different focal lengths *L*, following Reference [23], at operating wavelength $\lambda = 1.5\mu m$. (*P* indicates structure parameter, w_{eff} indicates fiber spot size and η_0 indicates coupling coefficient without misalignment)

$d^{/}$ = 6.0 μm, μ = 1.55

d/Λ	Λ (μm)	w_{eff} (μm)	L = 7.6 μm		L = 12.6 μm		L = 17.6 μm	
			P(μm)	η_0	P(μm)	η_0	P(μm)	η_0
0.35	2.3	2.805033	3.9	0.847159	6.0	0.482761	7.9	0. 286801
	3.0	2.969228	4.0	0.880081	6.2	0.519201	8.2	0.312642
	3.5	3.256532	4.1	0.927812	6.4	0.582515	8.6	0.359583
	4.0	3.628935	4.2	0.970748	6.6	0.661208	9.0	0.422344
	4.5	4.058139	4.2	0.995378	6.8	0.743838	9.2	0.495324
	5.0	4.490145	4.3	0.998423	6.8	0.816096	9.4	0.567315
0.40	2.3	2.310718	3.6	0.729077	5.2	0.376696	6.5	0.215833
	3.0	2.573870	3.8	0.795021	5.7	0.432000	7.3	0.252122
	3.5	2.869064	4.0	0.860238	6.1	0.496944	8.0	0.296780
	4.0	3.225618	4.1	0.923267	6.4	0.575772	8.6	0.354433
	4.5	3.625593	4.2	0.970448	6.6	0.660528	9.0	0.421773
	5.0	4.026105	4.2	0.994422	6.7	0.738035	9.2	0.489914
0.45	2.3	1.999448	3.2	0.649134	4.4	0.318155	5.4	0.179004
	3.0	2.301137	3.6	0.726516	5.2	0.374748	6.5	0.214600
	3.5	2.589569	3.8	0.798786	5.7	0.435414	7.4	0.254402
	4.0	2.924104	4.0	0.871401	6.1	0.509179	8.1	0.305460
	4.5	3.292278	4.1	0.932844	6.4	0.590240	8.6	0.365529
	5.0	3.660019	4.2	0.973449	6.6	0.667503	9.0	0.427649

Table 6 (b): Results for optimum coupling efficiency for a series of CCPCFs with different air filling ratio d/Λ and hole-pitch or lattice-constant Λ via QIML with different focal lengths *L*, following Reference [24], at operating wavelength $\lambda = 1.5\mu m$. (*P* indicates structure parameter, w_{eff} indicates fiber spot size and η_0 indicates coupling coefficient without misalignment)

$d' = 6.0\ \mu m$, $\mu = 1.55$

d/Λ	Λ (μm)	w_{eff} (μm)	$L = 8.19\mu m$		$L = 12.1875\mu m$		$L = 16.19\mu m$	
			P(μm)	η_0	P(μm)	η_0	P(μm)	η_0
0.35	2.3	2.805033	4.2	0.797345	5.8	0.505784	7.4	0.329184
	3.0	2.969228	4.3	0.833296	6.0	0.543075	7.6	0.357866
	3.5	3.256532	4.4	0.888228	6.2	0.607330	8.0	0.409503
	4.0	3.628935	4.5	0.942324	6.4	0.686441	8.3	0.477593
	4.5	4.058139	4.5	0.981306	6.5	0.768302	8.5	0.555204
	5.0	4.490145	4.6	0.998355	6.6	0.838702	8.7	0.630064
0.40	2.3	2.310718	3.8	0.673935	5.1	0.396536	6.2	0.249560
	3.0	2.573870	4.0	0.741737	5.5	0.453667	6.9	0.290436
	3.5	2.869064	4.2	0.811804	5.9	0.520353	7.5	0.340278
	4.0	3.225618	4.4	0.882767	6.2	0.600533	8.0	0.403865
	4.5	3.625593	4.5	0.941915	6.4	0.685762	8.3	0.476982
	5.0	4.026105	4.5	0.979275	6.5	0.762638	8.5	0.549516
0.45	2.3	1.999448	3.4	0.593903	4.4	0.335743	5.2	0.207711
	3.0	2.301137	3.8	0.671365	5.1	0.394499	6.2	0.248144
	3.5	2.589569	4.0	0.745581	5.6	0.457139	6.9	0.292993
	4.0	2.924104	4.2	0.823603	6.0	0.532787	7.6	0.349901
	4.5	3.292278	4.4	0.894339	6.2	0.615107	8.0	0.416003
	5.0	3.660019	4.5	0.946045	6.4	0.692720	8.3	0.483264

Table 7: Comparative results for optimum coupling coefficient η_0 and coupling loss CL_0 for CCPCFs with different air filling ratio d/Λ and hole-pitch or lattice-constant Λ excited with LD #1 and LD #2 for different focal lengths *L*. (*P* indicates structure parameter, and w_{eff} indicates fiber spot size)

$d' = 6.0\ \mu m$, $\mu = 1.55$

$\lambda = 1.3\ \mu m$						$\lambda = 1.5\ \mu m$				
L (μm)	d/Λ	Λ (μm)	w_{eff} (μm)	P (μm)	η_0 and CL_0 (dB)	d/Λ	Λ (μm)	w_{eff} (μm)	P (μm)	η_0 and CL_0 (dB)
7.6	0.35	3.5	3.071572	4.6	0.997630 0.0115	0.35	5.0	4.490145	4.3	0.998423 0.0068
8.19	0.45	4.5	3.236339	4.9	0.998334 0.0072	0.35	5.0	4.490145	4.6	0.998355 0.0071
12.1875	0.35	5.0	4.433909	7.0	0.996879 0.0136	0.35	5.0	4.490145	6.6	0.838702 0.7639
12.6	0.35	5.0	4.433909	7.2	0.993311 0.0291	0.35	5.0	4.490145	6.8	0.816096 0.8826
16.19	0.35	5.0	4.433909	9.0	0.906903 0.4244	0.35	5.0	4.490145	8.7	0.630064 2.0061
17.6	0.35	5.0	4.433909	9.7	0.858528 0.6624	0.35	5.0	4.490145	9.4	0.567315 2.4617